Pergamon

SCIENCE DIRECT®

Bioorganic & Medicinal Chemistry 11 (2003) 3945–3951

BIOORGANIC & MEDICINAL CHEMISTRY

Self-Organizing Molecular Field Analysis on α_{1a}-Adrenoceptor Dihydropyridine Antagonists

Minyong Li, Lüpei Du, Bin Wu and Lin Xia*

Department of Medicinal Chemistry, China Pharmaceutical University, Nanjing 210009, China

Received 25 February 2003; accepted 17 June 2003

Abstract—Self-organizing molecular field analysis (SOMFA), a new three-dimensional quantitative structure–activity relationship (3-D-QSAR) method is used to study the correlation between the molecular properties and theα_{1a}-AR biological activities of dihydropyridine derivatives. The statistical result, cross-validated q^2 (0.690) and non cross-validated r^2 (0.704) values, show a good predictive ability.

Introduction

Nowadays, the search for novel and selective α_1-adrenoceptor (α_1-AR) antagonists is increased due to their therapeutical potential in the treatment of hypertension and benign prostatic hyperplasia (BPH).[1]

The α_1-ARs mediate many effects of the sympathetic nervous system. Like other adrenergic receptors, α_1-ARs are activated by the catecholaimnes, adrenaline and noradrenaline. The α_1-ARs are member of the superfamily of seven transmembrane G-protein coupled receptors (GPCR).[2]

Pharmacological evidence and recent molecular cloning studies have demonstrated α_1-ARs are not a homogeneous population and three distinct α_1-AR subtypes, called α_{1A}, α_{1B} and α_{1D}, have been characterized by functional, radioligand binding and molecular biology studies.[2,3]

Some α_1-AR antagonists, such as terazosin and doxazosin,[4] are proven to relieve the symptoms of BPH so that are in clincial use. These α_1-AR antagonists, however, also have side effects which includes orthostatic hypotension, dizziness, impotence, and nasal congestion that may be in part due to cross-reaction of these compounds at the α_{1b} and α_{1d} receptor. Recent studies have demonstrated that the α_{1a}-AR subtype is the predominant receptor present in the prostate smooth muscle, and selective α_{1a}-AR antagonists will provide an advance in therapy for the treatment of BPH. Tamsulosin[5] was recently launched in the market as the first subtype selective α_{1a}-AR antagonists, and some new compounds, such as Silodosin (KMD-3213),[6] RS-97078[7] and B8805-033,[8] were reported to be under development for the treatment of BPH (Fig. 1).

S-(+)-Niguldipne, a dihydropyridine compound formerly investigated as an antihypertensive calcium channel blocker, exhibits a high affinity ($K_i = 0.2$ nM) binding to human α_{1a}-AR. Moreover, this compound shows 340- and 630-fold selectivity in binding to the cloned human α_{1a}-AR relative to the α_{1b}-AR and α_{1d}-AR, respectively.[9] Therefore, as a novel class of α_1-AR antagonists, dihydropyridine derivatives[9–12] (Table 1), have been studied for their potent and selective α_{1a}-AR antagonist activity. However, due to their weak α_{1b}-AR and α_{1d}-AR antagonist activities, here we only discuss their α_{1a}-AR antagonist activities.

The self-organizing molecular field analysis (SOMFA)[13] is a new 3-D-QSAR technique, which has been developed just recently by Robinson et al. The method has similarities to both comparative molecular field analysis (CoMFA)[14] and molecular similarity studies. Like CoMFA, a grid-based approach is used; however, no probe interaction energies need to be evaluated. Like the similarity methods it is the intrinsic molecular properties, such as the molecular shape and electrostatic potential, are used to develop the QSAR models.

*Corresponding author. Tel.: +86-253-271-440; fax: +86-253-301-638; e-mail: phenopro@cpu.edu.cn

0968-0896/03/$ - see front matter © 2003 Elsevier Ltd. All rights reserved.
doi:10.1016/S0968-0896(03)00410-3

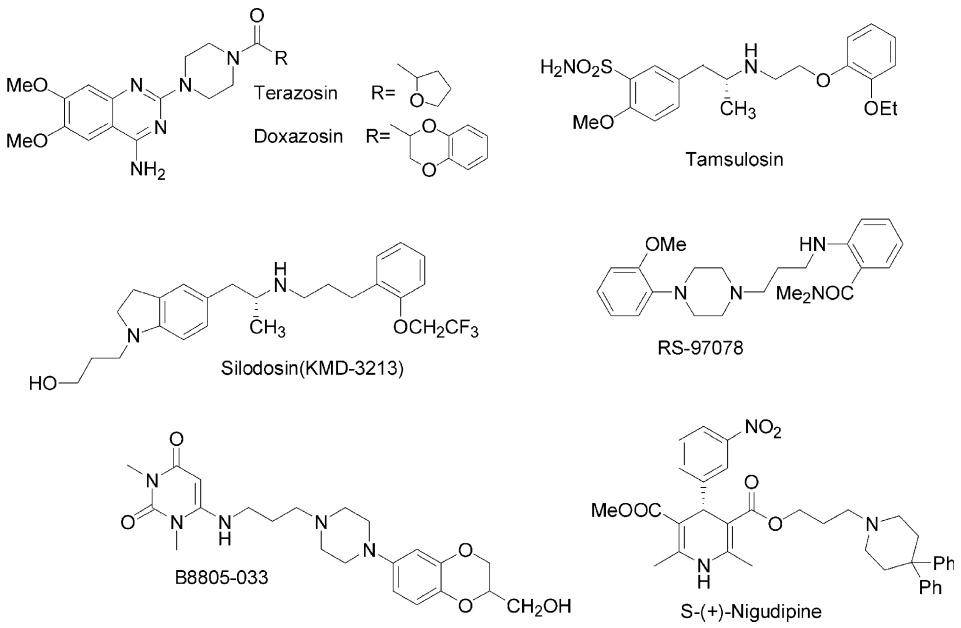

Figure 1. Chemical structures of some α_{1a}-AR antagonists.

A SOMFA model could suggest a method of tackling the all-important alignment, which all 3-D-QSAR methods have faced. The inherent simplicity of this method allows the possibility of aligning the training compounds as an integral part of the model derivation process and of aligning prediction compounds to optimize their predicted activities.

The purpose of this paper is to describe the application of self-organizing molecular field analysis, SOMFA, on a set of dihydropyridines, a novel class of α_{1a}-AR antagonists.

Methods

Data sets and biological activities (pK_i)

Sixty-three dihydropyridine compounds are divided into two sets. The training set of 50 molecules with structures and their α_{1a}-AR activities expressed as pK_i are shown in Table 1. The predictive power of the models is evaluated using a test set of 13 molecules whose structures and activities are also shown in Table 1. Two sets of 63 molecules are selected in order to find some molecular descriptors and to elucidate convenient models for the predictive discrimination between these various activities. All compounds and their activities are processed as enantiomers in order to decrease the molecular alignment error derived from different configuration and increase the correlation of SOMFA models.

Molecular modeling and alignment

The three-dimensional structures of the dihydropyridines are constructured with the HyperChem Release 7 Evaluation,[15] running on an Intel Pentium III 1066 MHz Processor/Microsoft WinXP Home Edition platform. Unless otherwise indicated, parameters are default. Full geometry optimization are performed first by molecular mechanics (MM+ force field, which modified from MM2 force field[16]) implemented in this software, then optimized and assigned charge by the AM1[17] and PM3[18] Hamiltonian semi-empirical method using the parameter set reported in the MOPAC.[19] The final geometries are then performed RMS overlapping and fitting. Three different three-atom alignments are selected to define overlay. The atom numbers and corresponding sequence for each alignment are listed in Table 2.

The compounds are then fitted to the template compound **1**, one of the most active compounds, according to the three alignment schemes. The alignments from best SOMFA model are shown in Figure 2. Using VEGA,[20] the final overlayed geometries are converted into CSSR file format, the only file format which SOMFA2 program can accept to process a SOMFA analysis.

SOMFA 3-D-QSAR models

In the SOMFA study a 40×40×40 Å grid originating at (−20, −20, −20) with a resolution of 0.5 and 1 Å, respectively, is generated around the aligned compounds. Table 3 reports 12 models using different alignment, charge and resolution of grid under exploration.

For all of the studies, shape and electrostatic potential are generated. To sum up the predictive power of these two properties into one final model, we combine their individual predictions using a weighted average of the shape and electrostatic potential based QSAR, using a mixing coefficient (c_1) as illustrated in eq 1.[12]

$$\text{Activity} = c_1\ \text{Activity}_{\text{shape}} + (1 - c_1)\ \text{Activity}_{\text{ESP}} \qquad (1)$$

Table 1. Chemical structures and corresponding α_{1a}-AR biological activities of the dihydropyridine compounds

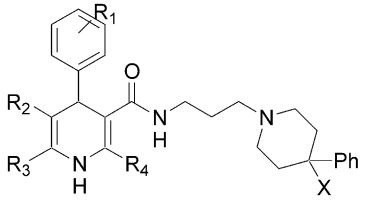

Compd[a]	R_1	R_2	R_3	R_4	X	Activities (pK_i)	Ref
1	4-NO_2	COOMe	CH_3	CH_3	Ph	9.46	9
2	4-NO_2	$CONH_2$	CH_3	CH_3	Ph	8.73	10
3	4-NO_2	CONHEt	CH_2CH_3	$(CH_2)_2CH_3$	Ph	8.42	10
4	4-NO_2	CONHEt	CH_2CH_3	$(CH_2)_4CH_3$	Ph	6.90	10
5	4-NO_2	$CONH_2$	CH_3	$(CH_2)_4NH_2$	Ph	8.36	10
6	4-NO_2	$CONH_2$	CH_3	$(CH_2)_3NH_2$	Ph	8.42	10
7	4-NO_2	$CONH_2$	CH_2CH_3	$CH_2OCH_2CF_3$	Ph	7.94	10
8	4-NO_2	$CONH_2$	CH_2CH_3	CH_2OCH_3	Ph	7.71	10
9	4-NO_2	$CONH_2$	CH_2CH_3	$(CH_2)_4OCH_3$	Ph	8.29	10
10	4-NO_2	$CONH_2$	CH_2CH_3	$CH_2O(CH_2)_3NH_2$	Ph	8.32	10
11	4-NO_2	$CONH_2$	CH_2CH_3	$CH_2O(CH_2)_2N_3$	Ph	8.48	10
12	4-NO_2	$CONH_2$	CH_2CH_3	$CH_2O(CH_2)_2NH_2$	Ph	9.30	10
13	4-NO_2	$CONH_2$	$CH_2O(CH_2)_3NH_2$	CH_2CH_3	Ph	8.77	10
14	4-NO_2	CONHEt	CH_2CH_3	$CH_2O(CH_2)_3NH_2$	Ph	8.35	10
15	4-NO_2	CONHEt	$CH_2O(CH_2)_3NH_2$	CH_2CH_3	Ph	8.52	10
16	4-NO_2	$CONH_2$	CH_3	$CH_2O(CH_2)_2NH_2$	H	8.86	10
17	4-NO_2	$CONH_2$	CH_3	$CH_2O(CH_2)_2NH_2$	4-OMe-Ph	8.20	10
18	4-NO_2	$CONH_2$	CH_3	$CH_2O(CH_2)_2NH_2$	COOMe	8.50	10
19	4-NO_2	$CONH_2$	CH_3	$CH_2O(CH_2)_2NH_2$	CH_2NMe_2	6.34	10
20	4-Cl	COOMe	CH_3	CH_3	Ph	8.75	11
21	4-CN	COOMe	CH_3	CH_3	Ph	8.74	11
22	4-OMe	COOMe	CH_3	CH_3	Ph	8.15	11
23	4-Me	COOMe	CH_3	CH_3	Ph	8.86	11
24	3,4-OCH_2O–	COOMe	CH_3	CH_3	Ph	8.95	11
25	3,4-Cl_2	COOMe	CH_3	CH_3	Ph	8.73	11
26	3-OMe-4-NO_2	COOMe	CH_3	CH_3	Ph	8.83	11
27	3,4-Benzo	COOMe	CH_3	CH_3	Ph	7.44	11
28	4-NO_2	COOMe	CH_3	CH_3	H	9.64	11
29	4-Cl-3-NO_2	COOMe	CH_3	CH_3	H	9.28	11
30	4-NO_2	CN	CH_3	CH_3	Ph	7.25	11
31	4-NO_2	COMe	CH_3	CH_3	Ph	8.93	11
32	4-NO_2	CONHMe	CH_3	CH_3	Ph	8.35	11
33	4-NO_2	$CONMe_2$	CH_3	CH_3	Ph	7.23	11
34	4-NO_2	$CONH_2$	CH_2CH_3	CH_2CH_3	Ph	8.97	11
35	4-NO_2	$CONH_2$	$CH(CH_3)_2$	$CH(CH_3)_2$	Ph	7.27	11
36	3,4-OCH_2O–	COMe	CH_3	CH_3	Ph	8.05	11
37	3,4-OCH_2O–	$CONH_2$	CH_3	CH_3	Ph	8.06	11
38	3,4-OCH_2O–	CONHMe	CH_3	CH_3	Ph	7.79	11
39	3,4-OCH_2O–	COOH	CH_3	CH_3	Ph	6.50	11
40	4-NO_2	$CONH_2$	CH_3	CH_3	CH_3	7.20	12
41	4-NO_2	$CONH_2$	CH_3	CH_3	COMe	7.57	12
42	4-NO_2	$CONH_2$	CH_3	CH_3	OH	8.11	12
43	4-NO_2	$CONH_2$	CH_3	CH_3	CN	8.54	12
44	4-NO_2	$CONH_2$	CH_3	CH_3	$CONMe_2$	6.34	12
45	4-NO_2	CONHMe	CH_3	CH_3	CH_2NMe_2	5.42	12
46	4-NO_2	$CONH_2$	CH_3	CH_3	COOMe	9.08	12
47	4-NO_2	$CONH_2$	CH_3	CH_3	COOEt	8.66	12
48	4-NO_2	$CONH_2$	CH_3	CH_3	$COO(CH_2)_2OMe$	8.27	12
49	4-NO_2	$CONH_2$	CH_3	CH_3	$COO(CH_2)_2OH$	8.04	12
50	4-NO_2	$CONH_2$	CH_3	CH_3	COOPh	8.22	12
51	4-NO_2	CONHMe	CH_3	CH_3	COOEt	8.21	12
52	4-NO_2	CONHMe	CH_3	CH_3	H	8.21	12
53	4-NO_2	CONHMe	CH_3	CH_3	COOMe	8.40	12
54	4-NO_2	$COO(CH_2)_2CN$	CH_3	CH_3	COOMe	8.32	12
55	4-NO_2	COOH	CH_3	CH_3	COOMe	7.23	12
56	4-NO_2	CONHEt	CH_3	CH_3	COOMe	8.32	12
57	4-NO_2	COOMe	CH_3	CH_3	COOMe	8.45	12
58	4-NO_2	COOEt	CH_3	CH_3	COOMe	8.43	12
59	4-NO_2	$COO(CH_2)_2OH$	CH_3	CH_3	COOMe	8.44	12
60	4-NO_2	COMe	CH_3	CH_3	COOMe	8.59	12
61	4-NO_2	COMe	CH_3	CH_3	COOEt	8.72	12
62	3,4-OCH_2O–	COMe	CH_3	CH_3	COOMe	8.38	12
63	3,4-OCH_2O–	$CONH_2$	CH_3	CH_3	COOEt	8.11	12

[a]Compounds **1**–**50**: training set; compounds **51**–**63**: test set.

Table 2. The atom numbers and three-atom sequences defining the three alignments; compound **1** (SNAP-5089) is used to define the atom numbering

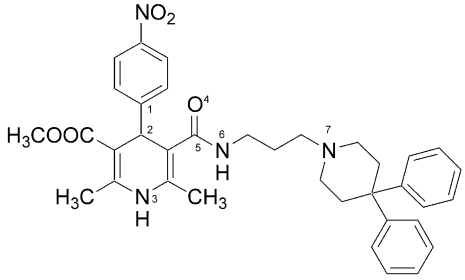

Alignment no.	1st atom	2nd atom	3rd atom
1	1	4	7
2	2	5	7
3	3	6	7

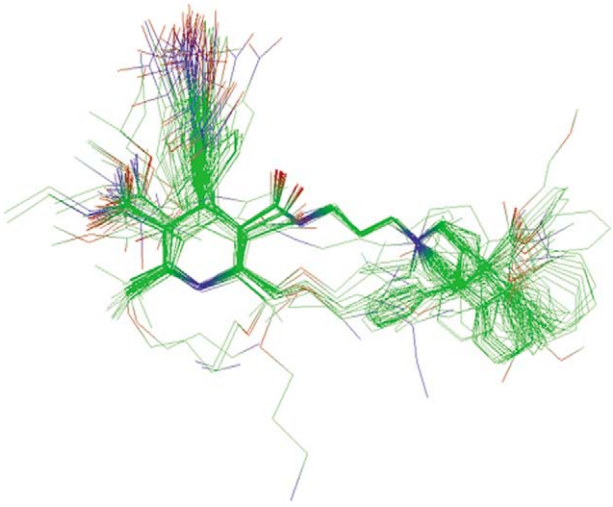

Figure 2. Superposition of all 63 compounds according to the optimized geometries and alignment 3. Hydrogens are removed for clarity.

Table 3. Encoding 12 models for the training set used for the SOMFA investigations

Model no.	Alignment no.	Charge	Resolution of grid (Å)
1	1	AM1	0.5
2	1	AM1	1
3	1	PM3	0.5
4	1	PM3	1
5	2	AM1	0.5
6	2	AM1	1
7	2	PM3	0.5
8	2	PM3	1
9	3	AM1	0.5
10	3	AM1	1
11	3	PM3	0.5
12	3	PM3	1

Clearly, multiproperty predictions could have been obtain through multiple linear regression. Using eq 1 instead gives greater insight into the resultant model by allowing the study of the variation in predictive power with different values of c_1.

With the highest value of r^2, the SOMFA models then are derived by the partial least squares (PLS), implemented in NoSA,[21] with cross-validation.

The predictive ability of the model is quantitated in terms of q^2 which is defined in eq 2:

$$q^2 = (\mathrm{SD} - \mathrm{PRESS})/\mathrm{SD}$$

$$\text{where } \mathrm{PRESS} = \sigma\left(Y_{\mathrm{pred}} - Y_{\mathrm{actual}}\right)^2$$

and

$$\mathrm{SD} = \sigma(Y_{\mathrm{actual}} - Y_{\mathrm{mean}})^2 \qquad (2)$$

SD is the sum of squares of derivations of the observed values from their mean and PRESS is the prediction error sum of squares. The final models are constructed by a conventional regression analysis with the optimum value of mixing coefficient (c_1) equal to that yielding the highest r^2 and q^2 value according to eq 2.

Table 4. Statistics of the various SOMFA models

Model	r^2	s	F	c_1	q^2
1	0.445	0.65	38.47	0.0	0.444
2	0.437	0.65	37.28	0.1	0.435
3	0.227	0.77	14.09	0.0	0.226
4	0.235	0.76	14.76	0.0	0.234
5	0.612	0.55	72.65	0.0	0.597
6	0.583	0.56	67.23	0.0	0.554
7	0.305	0.72	21.85	0.0	0.313
8	0.322	0.72	22.77	0.0	0.314
9	**0.704**	**0.47**	**114.02**	**0.3**	**0.690**
10	0.703	0.48	113.58	0.3	0.689
11	0.470	0.64	42.58	0.3	0.466
12	0.483	0.63	44.78	0.4	0.480

r^2, Non cross-validated correlation coefficient; s, standard error of estimate; F, F-test value; c_1, mixing cofficient of SOMFA model; q^2, Cross-validated correlation coefficient.

Table 5. Observed and predicted activities of 50 compounds in the training set

Compd	Observed	Predicted	Residual[a]
1	9.46	9.62	−0.16
2	8.73	9.53	−0.8
3	8.42	7.9	0.52
4	6.9	7.73	−0.83
5	8.36	7.87	0.49
6	8.42	7.91	0.51
7	7.94	7.73	0.21
8	7.71	7.9	−0.19
9	8.29	7.92	0.37
10	8.32	8.19	0.13
11	8.48	8.29	0.19
12	9.3	9.18	0.12
13	8.77	8.41	0.36
14	8.35	8.23	0.12
15	8.52	8.08	0.44
16	8.86	8.88	−0.02
17	8.2	8.05	0.15
18	8.5	8.55	−0.05
19	6.34	6.49	−0.15
20	8.75	8.66	0.09
21	8.74	8.74	0
22	8.15	8.76	−0.61
23	8.86	7.99	0.87
24	8.95	9.24	−0.29
25	8.73	8.13	0.6
26	8.83	8.47	0.36
27	7.44	7.87	−0.43
28	9.64	9.63	0.01
29	9.28	8.42	0.86
30	7.25	7.87	−0.62
31	8.93	7.93	1
32	8.35	7.91	0.44
33	7.23	7.89	−0.66
34	8.97	8.81	0.16
35	7.27	8.14	−0.87
36	8.05	7.79	0.26
37	8.06	7.95	0.11
38	7.79	7.9	−0.11
39	6.5	6.83	−0.33
40	7.2	7.81	−0.61
41	7.57	8	−0.43
42	8.11	7.89	0.22
43	8.54	8.2	0.34
44	6.34	5.87	0.47
45	5.42	5.62	−0.2
46	9.08	8.11	0.97
47	8.66	7.83	0.83
48	8.27	7.99	0.28
49	8.04	7.94	0.1
50	8.22	7.84	0.38

[a]Residual = Observed − predicted.

Since the final equations are not very useful to represent efficiently the SOMFA models, 3-D master grid maps of the best model are displayed by program Grid-Visualizer. They represent areas in the space where steric and electrostatic field interaction are responsible for the observed variations of the biological activity.

Results and Discussion

SOMFA, a novel 3-D-QSAR methodology, is employed for the analysis with the training set composed of 50 various compounds, which biological activities are known. Statistical results of 12 SOMFA models are summarized in Table 4.

Table 6. Observed and predicted activities of 13 compounds in the test set

Compd	Observed	Predicted	Residual[a]
51	8.21	7.91	0.30
52	8.21	7.91	0.30
53	8.40	9.04	−0.64
54	8.32	8.13	0.19
55	7.23	7.76	−0.53
56	8.32	8.08	0.24
57	8.45	8.21	0.24
58	8.43	8.13	0.30
59	8.44	8.17	0.27
60	8.59	8.10	0.49
61	8.72	7.84	0.88
62	8.38	7.72	0.66
63	8.11	7.95	0.16

[a]Residual = Observed − predicted.

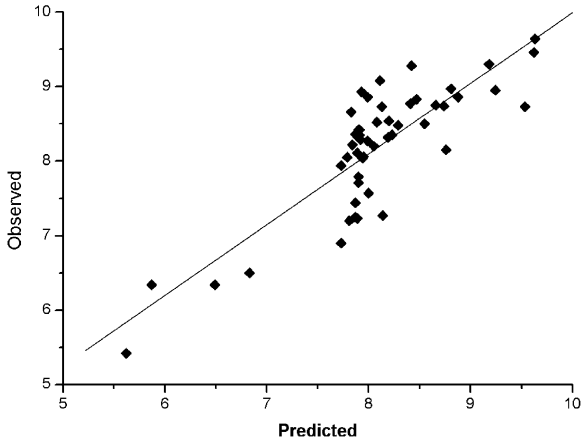

Figure 3. Observed versus predicted α_{1a}-AR antagonist activities in the training set.

A cross-validated value q^2 which is obtained as a result of PLS analysis serves as a quantitative measure of the predictability of the SOMFA model. From the table we find that the result is less sensitive to resolution of grid and quantum mechanics optimization but the model overlayed using alignment 3 shows higher q^2 values than using the others.

Among the twelve models tested, the best predictive power is the ninth models from cross-validated. Good cross-validated correlation coefficient q^2 values (0.690), moderate non cross-validated correlation coefficient r^2 values (0.704) proves a good conventional statistical correlation have been obtained, and we also find that the resultant SOMFA model have a fair predictive ability.

During the SOMFA investigation, grid spacings of 1 and 0.5 Å were investigated. The 1 Å grid spacing produces a good correlation equal to 0.5 Å grid. This improved marginally with the 0.5 Å spacing uses for the results presented here. Further increases in resolution produced further small increases in model quality but not enough to warrant the extra computational time.

The observed and predicted activities of the training set are reported in Table 5. Figure 3 shows a good linear

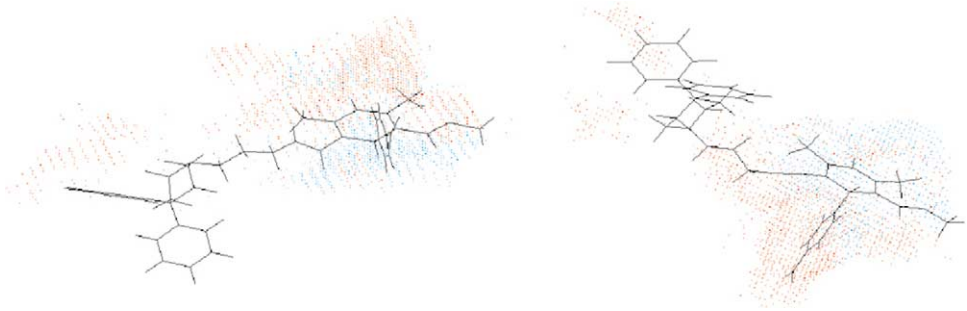

Figure 4. The electrostatic potential master grid with compound **1** from two different viewpoints. Red represents areas where postive potential is favorable, or negative charge is unfavorable. Blue represents areas where negative potential is favorable, or postive charge is unfavorable.

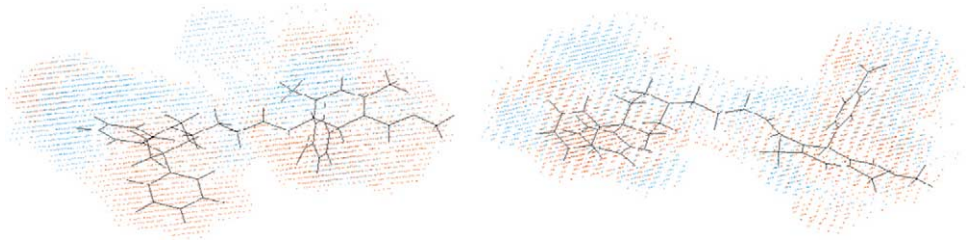

Figure 5. The shape master grid with compound **1** from two different viewpoints. Red represents areas of favorable steric interaction. Blue represents areas of unfavorable steric interaction.

correlation and moderate difference between observed and predicted values of molecules in the training set.

It's well known that the best way to validate a 3-D-QSAR model is to predict biological activities for some compounds of test set. The SOMFA analysis of the test set composed of 13 compounds is reported in Table 6. Most of compounds in test set show good correlation between observed and predicted values.

SOMFA calculation for both shape and electrostatic potentials are performed then combined to get an optimal coefficient $c_1 = 0.3$ according to eq 1. The master grid maps derived from the best model is used to display the contribution of electrostatic potential and shape molecular field. The master grid maps give a direct visual indication of which parts of the compounds differentiate the activities of compounds in the training set under study. The master grid also offer an interpretation as to how to design and synthesis some novel compounds with much higher activities. The visualization of the electrostatic potential master grid and shape master grid of the best SOMFA model is showed in Figures 4 and 5, respectively, with compound **1** as the reference.

Each master grid map is colored in two different colors for favorable and unfavorable effects. In other words, the electrostatic features are red (more positive charge increases activity, or more negative charge decreases activity) and blue (more negative charge increases activity, or more positive charge decreases activity), and the shape feature are red (more steric bulk increases activity) and blue (more steric bulk decreases activity), respectively.

SOMFA analysis result indicates the electrostatic contribution is of high importance ($c_1 = 0.3$). The SOMAF electrostatic potential for the analysis is presented as master grid in Figure 4. In this map of important features, we find a high density of red points around the substituent R_3 and R_4 at the dihydropyridine ring, and around the *o* and *m* position at the phenyl ring, which means some electropositive groups are favorable. We also find a high density of blue points around the *p* position at the phenyl ring, and around the substituent R_2 at the dihydropyridine ring, which means some strong electronegative groups are favorable.

Meanwhile, in the map of shape master grid, we can find a high density of red points around the substituent R_2 at the dihydropyridine ring, and around the *p* position at the phenyl ring, which means a favorable steric interaction; simultaneously, we find a high density of blue points around the substituent R_3 and R_4 at the dihydropyridine ring, and around the *o* and *m* position at the phenyl ring, which means a unfavorable steric interaction. In the area of substituent X neighboring to a phenyl ring we find a cluster of blue points, where an unfavorable steric interaction may be expected to enhance activities.

All analysis of SOMFA model may provide some useful information in the design of new dihydropyridine α_{1a}-AR antagonists.

Conclusion

We have developed predictive SOMFA 3-D-QSAR models for dihydropyridines as α_{1a}-AR antagonist. The master grid obtained for the various SOMFA models electrostatic potential contributions can be mapped back onto structural features relating to the trends in activities of the molecules. On the basis of the spatial

arrangement of the various electrostatic potential contributions, novel molecules are being designed with improved activity.

Acknowledgements

We are grateful for the help of Mr Michael J. Sorich, a PhD candidate from School of Pharmaceutical, Molecular and Biomedical Sciences, University of South Australia. We also gratefully acknowledge Dr Daniel Robinson and the Computational Chemistry Research Group (Oxford University, UK) for the use of the SOMFA software. This work is supported by the National High-Tech Research and Development Plan (National 863 Plan) under grant No. 2002AA2Z3118.

References and Notes

1. Chess-Williams, R. *Expert Opin. Pharmacother.* **2002**, *3*, 167.
2. Bylund, D. B.; Eikenberg, D. C.; Hieble, J. P.; Langer, S. Z.; Lefkowitz, R. J.; Minneman, K. P.; Molinoff, P. B.; Ruffolo, R. R., Jr.; Trendelenburg, U *Pharmacol. Rev.* **1994**, *46*, 121.
3. Hieble, J. P.; Bylund, D. B.; Clarke, D. E.; Eikenburg, D. C.; Langer, S. Z.; Lefkowitz, R. J.; Minneman, K. P.; Ruffolo, R. R. *Pharmacol. Rev.* **1995**, *47*, 267.
4. Thiyagarajan, M. *Pharmacology* **2002**, *65*, 119.
5. Chapple, C.; Andersson, K. E. *World J. Urol.* **2002**, *19*, 397.
6. Shibata, K.; Foglar, R.; Horie, K.; Obika, K.; Sakamoto, A.; Ogawa, S.; Tsujimoto, G. *Mol. Pharmacol.* **1995**, *48*, 250.
7. Elworthy, T. R.; Ford, A. P. D. W.; Bantle, G. W.; Morgans, D. J., Jr.; Ozer, R. S.; Palmer, W. S.; Repke, D. B.; Romero, M.; Sandoval, L.; Sjogren, E. B.; Talamás, F. X.; Vazquez, A.; Wu, H.; Arredondo, N. F.; Blue, D. R., Jr.; DeSousa, A.; Gross, L. M.; Kava, M. S.; Lesnick, J. D.; Vimont, R. L.; Williams, T. J.; Zhu, Q.-M.; Pfister, J. R.; Clarke, D. E. *J. Med. Chem.* **1997**, *40*, 2674.
8. Eltze, M.; Boer, R.; Michel, M. C.; Hein, P.; Testa, R.; Ulrich, W. R.; Kolassa, N.; Sanders, K. H. *Naunyn Schmiedebergs Arch. Pharmacol.* **2001**, *363*, 649.
9. Wetzel, J. M.; Miao, S. W.; Forray, C.; Borden, L. A.; Branchek, T. A.; Gluchowski, C. *J. Med. Chem.* **1995**, *38*, 1579.
10. Marzabadi, M. R.; Hong, X.; Nagarathnam, D.; Miao, S.; Chiu, G.; Wong, W. C.; Wetzel, J. M.; Fang, J.; Forray, C.; Chen, T. B.; O'Malley, S. S.; Chang, S. L.; Cluchowski, C. *Bioorg. Med. Chem. Lett.* **1999**, *9*, 2843.
11. Wong, W. C.; Chiu, G.; Wetzel, J. M.; Marzabadi, M. R.; Nagarathnam, D.; Wang, D.; Fang, J.; Hong, X.; Forray, C.; Vaysse, P. J.; Branchek, T. A.; Cluchowski, C. *J. Med. Chem.* **1998**, *41*, 2643.
12. Nagarathnam, D.; Wetzel, J. M.; Miao, S. W.; Marzabadi, M. R.; Chiu, G.; Wong, W. C.; Hong, X.; Fang, J.; Forray, C.; Branchek, T. A.; Heydorn, W. E.; Chang, S. L.; Borten, T.; Schorn, T. W.; Cluchowski, C. *J. Med. Chem.* **1998**, *41*, 5320.
13. (a) Robinson, D. D.; Winn, P. J.; Lyne, P. D.; Richards, W. G. *J. Med. Chem.* **1999**, *42*, 573. (b) SOMFA2 v2.0.0, a novel suite of programs which can carry out an advanced 3-D-QSAR analysis of a series of molecules, can be downloaded from author's homepage: http://bellatrix.pcl.ox.ac.uk. (c) Robinson, D. D. *SOMFA2 Instruction Manual*; New Chemistry Laboratory: Oxford University, UK, 1999.
14. Cramer, R. D., III; Patteerson, D. E.; Bunce, J.D *J. Am. Chem. Soc.* **1988**, *110*, 5959.
15. *HyperChem Release 7 Evaluation*; Hypercube Inc., 2002, which can be free downloaded from: http://www.hyper.com as a 30-day evaluation copy.
16. Allinger, N. L. *J. Am. Chem. Soc.* **1977**, *99*, 8127.
17. Dewar, M. J. S.; Zoebisch, E. G.; Healy, E. F.; Stewart, J. J. P. *J. Am. Chem. Soc.* **1985**, *107*, 3902.
18. Stewart, J. J. P. *J. Comput. Chem.* **1989**, *10*, 209.
19. Stewart, J. J. P. J. *Computer-Aided Mol. Des.* **1990**, *4*, 1.
20. (a) Pedretti, A.; Villa, L.; Vistoli, G. *J. Mol. Graph. Model.* **2002**, *21*, 47. (b) VEGA Release 1.4.2.7, a versatile program to convert, handle and visualize molecular structure on Windows-based PCs; its executable and the source code can be free downloaded from: http://users.unimi.it/ddl
21. NoSA V2.30 Build 2003.02.11, a statistics software with simply interface, which can be downloaded from its homepage: http://nosa.myrice.com as a shareware.